2007 IEEE International Conference on
Robotics and Automation
Roma, Italy, 10-14 April 2007

Electrolytic Silicone Bourdon Tube Microactuator for Reconfigurable Surgical Robots

Nicola Ng Pak*, Robert J. Webster III†, Arianna Menciassi*, and Paolo Dario*

Abstract— **Many compelling future surgical applications will be enabled by a new kind of surgical tool, capable of entering the human body through natural orifices or very small incisions and then reconfiguring into complex kinematic structures at the site of intervention. We describe a first step toward this goal - the development of a microactuator designed for use in surgical robots that are composed of large quantities of reconfigurable micro-robotic modules. The miniaturizable design proposed harnesses the Bourdon effect to convert electrolytic pressure into mechanical motion obtaining more than 400% displacement variation while consuming less than 0.5 W at less than 5 V. We describe the design, construction, and experimental results with our prototype microactuator.**

I. INTRODUCTION

Large robots for minimally invasive surgery (MIS) are already at the clinical stage (e.g. Da Vinci robot by Intuitive Surgical Inc., Mountain View CA, Zeus system by Computer Motion Inc., Santa Barbara, CA) and current research is devoted to integrating the most powerful technologies in terms of imaging, diagnostics tools, etc., into existing systems [1], [2], [3]. These machines are designed to operate in small and delicate workspaces by ensuring high accuracy, reducing operator fatigue, and reducing the performance gap between the best and worst surgeons. It is unlikely that the present generation of robots for MIS will dominate future surgical practice. Recent analysis based on a broad review of the field suggests that surgical robots should evolve toward hand-held and endoluminal systems [4] to achieve greater impact on medicine.

In keeping with this, our research aims to enable extremely targeted, localized and high precision endoluminal surgery. This requires an entirely new type of surgical tool, capable of entering the human body as a group of individual micromodules through natural orifices or very small incisions, and then assembling into complex reconfigurable kinematic structures at the site of the surgical intervention. Self-assembly allows the larger robot structure to pass through the smallest possible entry port, potentially sparing healthy tissue. Reconfigurability makes the system adaptable to a variety of surgical sites and objectives. The stomach is an example of a surgical site that is ideal for modular robots because the least invasive entry path (the esophagus) is much smaller than the surgical environment itself. We aim to create a clinically useful reconfigurable robot for the stomach by designing a set of swallowable modules. The stomach offers large free volume (up to 1000 cm^3) with muscular elastic walls that are not easily damaged. Constraints on dimensions of the modules are given by the esophagus. While the size of the esophagus varies from person to person, even the smallest people can swallow a cylindrical pill-shaped capsule 4 mm in diameter by 8 mm in length. Further, approximately 80% of people can swallow a capsule 10 mm in diameter by 20 mm long [5].

This small module size requires reducing the size of many robotic components. We propose a system composed of several modules, each with different distinct functions (e.g. power modules, actuation modules, communication modules, and end-effector modules). In this paper we present our work toward creating an actuation module as a proof of concept and starting point for the development of a swallowable self-assembling reconfigurable robot.

II. DESIGN AND MODELLING

Development of a new microactuator is motivated by the large size of current reconfigurable modular robots. A good survey of the current state of the art can be found in [6], which reports that even the smaller reconfigurable robot modules developed to date are $40 \times 40 \times 80$ mm^3, which is clearly much too large for our application. Electric motors are similarly too large. Thus, alternative actuation principles must be investigated, as in [7] where SMA is employed to reduce module size to 30 mm.

Power is likely to be a limiting factor in a modular reconfigurable robot design, so it is desirable for actuators to consume as little power as possible. In the field of innovative actuators working at low voltage (important for both power consumption and safety) electrolytic actuation seems the most promising as reported in [8], where the gases produced by the decomposition of water were employed to drive a 3.6 cm^2 piston. Converting liquids like water to gas creates a source of pressure without consuming much electrical power or requiring pumping mechanisms.

We have designed a device to exploit the pressure produced creating mechanical displacement via the Bourdon effect. The Bourdon effect arises as a curved hollow tube with an elliptical cross section is inflated. As the internal pressure increases the cross section becomes more circular,

Manuscript received September 15, 2006. This work was supported in part by the European Commission in the framework of the 6FP NEST-Adventure Project ARES (Assembling Reconfigurable Endoluminal Surgical system), as well as by the National Science Foundation Graduate Research Fellowship supporting Robert Webster.

†Robert Webster is with the Department of Mechanical Engineering, The Johns Hopkins University, 3400 North Charles Street, Baltimore, Maryland 21218, USA robert.webster@jhu.edu

*Nicola Ng Pak, Arianna Menciassi, and Paolo Dario are with the Scuola Superiore Sant'Anna, Crim Lab, viale Rinaldo Piaggio 34, 56025 Pontedera (PI) - Italy. ngpak@crim.sssup.it, arianna@sssup.it, dario@sssup.it

causing the tube to straighten and displacing the tip. We have developed a Silicone Bourdon Tube (SBT) actuator connected to a box filled with an electrolytic salt water solution. Inside the box electric current passes through the solution, decomposing water into oxygen and hydrogen gas. These mixed gases pressurize the interior of the SBT. Silicone (RTV-Tixo, Prochima S.n.c.) has been selected for its natural compliance and high deformability, which allow us to build a compact actuator with small initial radius of curvature.

A. Electrolysis

The reactions taking place inside the box are:

$$\begin{array}{l} 4H_2O + 4e^- \rightarrow 2H_{2(g)} + 4OH^- \\ \underline{6H_2O \rightarrow O_{2(g)} + 4H_3O^+ + 4e^-} \\ 2H_2O \rightarrow 2H_2 + O_2, \end{array} \quad (1)$$

with a neutral salt solution.

The process requires 1.23 Volts at 25° C and 1 atm (plus an overpotential due to secondary effects at the electrodes). Assuming the ideal gas law ($PV = nRT$) holds, such gas production will theoretically provide a maximum strain of 136000% at constant pressure and a maximum pressure of 200 MPa at constant volume [8]. Another interesting characteristic of water electrolysis is the scalability of the process, making it suitable for MEMS applications [9]. This feature, combined with the high strain achievable, enables design of very compact micro-size, long stroke actuators.

B. The Bourdon Tube

The Bourdon tube is commonly used as a pressure transducer. It is normally composed of a hollow tube of elliptical cross section, made from relatively soft metals, closed at one end, and curved in a semi-circular shape. Pressurization of the inside of the Bourdon tube induces a change in curvature due to the deformation of the cross-section toward a circular shape.

Since Eugene Bourdon originally patented the Bourdon tube more than 150 years ago, and because of its ubiquitous use in pressure gauges (due to nearly linear tip motion for small displacements), one might expect to find well-developed analytical models in the literature. Interestingly, such analytical models have not yet been developed, and there are also many open research questions in numerical approaches. Even pressure gauge manufacturers develop and customize new pressure gauges without using good models, resorting to design solely on the basis of adapting previous "tried and true" designs to new requirements and using experimental adjustment to calibrate the final gauge [10].

In this paper we derive a simple idealized model relating the pressure and the radius of curvature, which fits our device performance well over the range of pressures (and corresponding radii) in our experiments, in the range of 0-100 kPa. We make three assumptions in our model, (1) the cross-sections remain perpendicular to the axis of the tube, (2) the length (L) of the tube is constant, and (3) the volume of the Bourdon tube can be approximated as the product

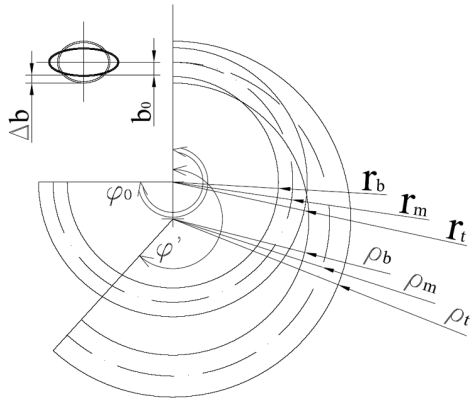

Fig. 1. Geometry of the Bourdon Tube in its rest (radii denoted with r and pressurized (radii denoted with ρ) states.

of the cross section area and the length, L. Taken together, assumptions (1) and (2) imply that the length of the top and bottom surfaces of the tube (L_t and L_b) remain constant. Assumption (3) simplifies the calculation of volume inside the tube. From the geometry of Fig. 1, we can write down the relationships,

$$\begin{cases} \rho_b/L_b = \rho_t/L_t \quad \text{and} \\ \rho_t - \rho_b = 2(b_0 + \Delta b), \end{cases} \quad (2)$$

where b_0 is the initial half minor axis of the ellipse, Δb is the half minor axis variation due to inflation, and ρ_b, ρ_m, and ρ_t are the respective the radii of curvature of the bottom, midline, and top surfaces of the pressurized Bourdon tube.

Since $\rho_m = \frac{\rho_b + \rho_t}{2}$, substitution yields,

$$\rho_m = (b_0 + \Delta b)\frac{L_t + L_b}{L_t - L_b}, \quad (3)$$

which shows ρ_m is a function of initial constants and only one variable, Δb. Note that L_b cannot equal L_t.

Given that ρ_m is a function of only Δb, we must define the relationship between the pressure inside the tube (p) and Δb. Fig. 2 shows the elliptical Bourdon tube cross section with arrows indicating the direction of pressure. To simplify modeling we approximate the top and bottom surfaces of the Bourdon tube as flat, and lateral sides at higher curvature as linear springs as shown in Fig. 2. This is a good approximation for the SBT described in Section III, when it is deflated or slightly inflated. This model comes from the consideration that the main stresses arise at the highly curved sides, as shown in a FEM simulation performed using ANSYS™ (Fig. 3). The simulation carried out refers to a simple example, assuming a metallic Bourdon tube and using linear elastic isotropic elements. However, the Young's Modulus used was that experimentally acquired for the particular silicone used in our SBT, Υ = 242 kPa.

The integral of the vertical pressure components on one half of the ellipse (cut by the major axis) leads to a total force of $P = 2pa_0$. Then the width of the simplified cross-section with flat surfaces is set to $2a_0$ in order to obtain the same total vertical force integrating the pressure p over the flat area.

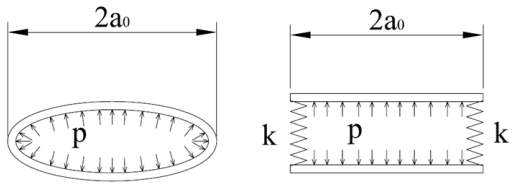

Fig. 2. Simplified cross sectional model. For a SBT with low inflation the top and bottom surfaces are nearly flat, while the sides have very high curvature.

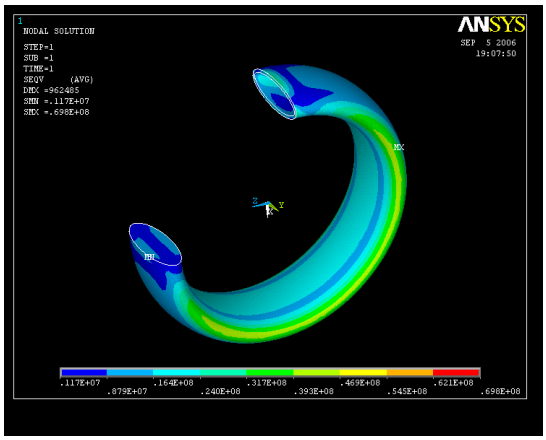

Fig. 3. An ANSYS FEM simulation reveals highest stress on the highly curved sides of the SBT profile.

Thus,

$$p = \frac{2K\Delta b}{2a_0}. \tag{4}$$

Substituting (4) into (3),

$$\rho_m = \left(\frac{L_t + L_b}{L_t - L_b}\right)\frac{a_0}{K}p + b_0\left(\frac{L_t + L_b}{L_t - L_b}\right) \tag{5}$$

This model for the pressurized radius of curvature of the SBT depends on the lumped parameter K which will be experimentally determined.

III. SBT FABRICATION

To verify the models of the electrolytically actuated SBT presented above, we have constructed a small, bio-compatible Bourdon tube and an associated electrolysis box. While this first SBT prototype is larger than what we envision in a final clinical system, it is specifically designed to be amenable to miniaturization by customized fabrication techniques . It serves as a proof of concept, showing that it is possible to create a small, low-power, electrolytically actuated Bourdon tube that inflates in a reasonable time period.

As the base material for the Bourdon tube we selected RTV-Tixo silicone (from Prochima S.n.c.). After full polymerization the material has natural compliance (shore A hardness = 25) which decreases the probability of trauma to the human body. Similar soft materials exist which have been demonstrated to be bio-compatible.

The other main component of our SBT is a small air chamber in the shape of a cylindrical plastic bag, 4.5 mm in diameter by 50 mm long. This was manufactured by winding a plastic sheet (LDPE) around a $\phi = 4.5$ *mm* metal rod and sealing the edge and one end with thermal treatments. The other end was attached using cyanoacrylate and primer to a TYGON® tube (S-50-HL, $\phi = 5/32$ in.) to provide a pressure inlet that would elastically seal to an outlet on the electrolysis box.

To create the curved shape of the SBT, we began by forming a thin sheet of RTV-Tixo, approximately 1 mm thick, and allowing it to polymerize. This sheet was then stretched between two clamps (as shown in Fig. 4, I), and the flattened air chamber was placed on top of it. Liquid RTV-Tixo was then spread over the top of both the first layer and the air chamber (Fig. 4, II) and allowed to polymerize. As it polymerized, it formed a bond with the first layer of silicone, making the two indistinguishable as separate entities. When the clamps were released and the excess silicone cut away, the pre-tension on the first layer causes the silicone and embedded plastic air chamber to roll into the bourdon tube shape as shown in Fig. 4, III). By changing the amount of pre-tension, one can manufacture SBTs with different radii of curvature. The final device is contained in a volume of $30 \times 27 \times 10$ mm^3 (excluding the inlet tube), and the final thickness is 2 mm and the radius of curvature is 7.50 mm (Fig. 5). While this is the rest size of the SBT prototype, it can be coiled tighter to fit within a much smaller package if desired.

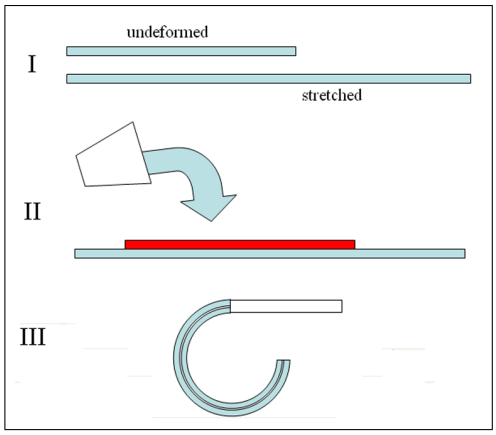

Fig. 4. (I) The bottom silicon sheet is first stretched and fixed in place. (II) The plastic pressure chamber is collapsed, laid on the membrane, and covered with liquid silicone, which is allowed to polymerize. (III) Releasing the tension on the bottom sheet causes the device to roll into a bourdon tube configuration.

For generating electrolytic pressure a box with interior dimensions of $20 \times 20 \times 15$ mm^3 was fabricated by rapid prototyping. A $\phi = 4$ *mm* outlet was included for attaching the TYGON® tube. Two platinum electrode wires (ϕ = 0.5 mm), were inserted through small holes in the wall of the box and sealed with cyanoacrylate. The box can be filled with an electrolytic solution through a sealable inlet, which also serves as the connection point for a pressure measurement device. The complete system is pictured in Fig. 6,b).

Fig. 5. The SBT prototype.

IV. EXPERIMENTAL RESULTS

Two different sets of experiments were carried out evaluating SBT shape, along with a force experiment. In the first set of shape experiments as well as the force experiment, the performance of the SBT was evaluated while it was pressurized using air from a syringe. In the second set, the electrolysis box generated the input pressure. The first experimental setup is composed of (1) the SBT (fabricated as described above), (2) a digital pressure sensor (SPER SCIENTIFIC, mod. 840081, pressure range 0-15 psi), (3) a syringe connected to the SBT by TYGON® tubing and (4) a camera used to record curvature and pressure.

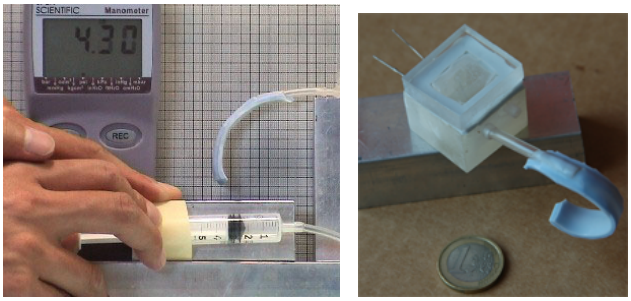

(a) (b)

Fig. 6. (a) The experimental setup for the syringe actuated SBT, (b) The electrolysis chamber connected to the SBT.

A. SBT Extension Experiment

The pressure sensor's digital display was placed in the view of a digital video camera along with the SBT. Behind the SBT was placed a physical grid to enable extraction of radius of curvature. Thus camera images contained time synchronized pressure and curvature information. By manually actuating the syringe plunger, several pressure cycles were performed and the extension of the SBT was recorded (Fig. 6,a)). The radius of curvature was extracted from the video images by manually finding the best-fit circle. We estimate the error in this data collection procedure to be $\pm 5\%$, due largely to slight variation in curvature along the tube. As can be seen plotted in diamond shapes on Fig. 8, the measured results are approximately linear ($R^2 = 0.91$), in accordance with the model proposed in Section II.

B. Force Experiment

To investigate whether the SBT is capable of applying clinically useful levels of force, we performed a second experiment. We placed a scale near the SBT with its flat surface tangential to the SBT's curvature, and positioned so that the point of contact would be located near the tip of the SBT. A force of approximately 120 mN was recorded at a pressure of 56 kPa and a first-sensor-contact radius of curvature of 12 mm. It should be noted that because this was a non-destructive test, a higher force is achievable simply by increasing the pressure inside the chamber. Moreover forces may be quite different depending upon the actual curvature and where they are measured (e.g. the tip vs. various points along the SBT), as well as the direction in which they are measured.

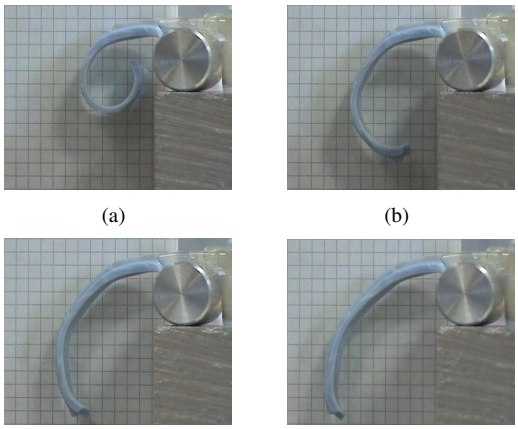

(a) (b) (c) (d)

Fig. 7. Images of the SBT changing shape as it is pressurized via electrolysis.

C. Electrolysis Actuated SBT

Pressure was generated via electrolysis for a second set of experiments. A power supply was connected to the electrolytic pressure box, and digital readouts were again arranged in the camera frame to provide time-synchronized recordings of (1) the current coming from the power supply, (2) SBT curvature, and (3) the pressure within the SBT. The power supply was connected to the platinum electrodes of the electrolytic box. The box itself is filled with a 0.5M solution of K_2SO_4 – a strong electrolyte that reduces the resistance of the water. This salt is not consumed during electrolysis (and thus is re-usable over multiple cycles), and is bio-compatible. No tissue damage will result in case of unexpected fluid escape [11]. The current of the power supply was set to 100 mA and the voltage to 4.9 V. Images of the inflation sequence of the electrolytically actuated SBT is shown in Fig. 7.

In Fig. 8 the electrolysis actuated SBT data is shown together with data taken when pressurizing the SBT via syringe. Note that both are approximately linear ($R^2 = 0.93$ for electrolysis, $R^2 = 0.91$ for syringe), with slight deviations in the data from linear at the lower and and upper bounds of the pressure used in the experiments. This behavior is probably due to non-linearities created by the interaction between the plastic bag and the encapsulating silicone.

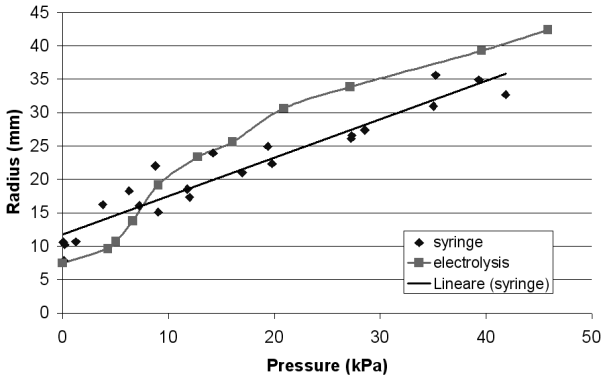

Fig. 8. The approximately linear relationship between the radius of curvature and the pressure applied to the SBT by a syringe is shown in diamond symbols. The least squares linear fit is $\rho_b = 0.57p + 11.78$ with R^2=0.91. The squares symbols represent the behavior of the SBT when pressurized by the electolysis, demonstrating a similar linear relationship with R^2 = 0.93.

Fig. 9 also shows the radius of curvature with respect to time, demonstrating that an extension movement of the SBT takes only a few seconds, even at the low power used in this experiment. The velocity of radius change is 0.43 mm/s.

The maximum radius of curvature is reached after 89 s, producing $7.74 \cdot 10^{-5}$ moles of gases at 100 mA and 4.9 V. These particular numbers are based on the resistance of the electrolyte solution and the resistance (and consequently power consumed) can be lowered by increasing the salt concentration or decreasing the distance between the electrodes. The energy consumed is 46.3 J spent in (1) producing the electrolysis reaction (approximately 14.2 J, given the reaction energy of 286 kJ per mole of H_2O), (2) heat production, and (3) deforming the SBT. The energy absorbed by the electrolysis reaction represents a limit for efficiency, which in our prototype is of 69.3%. Optimization of power consumption is a topic for future study. For our current purposes it is enough to establish that electrolysis can pressurize even a large prototype SBT with low power consumption in a relatively short time period.

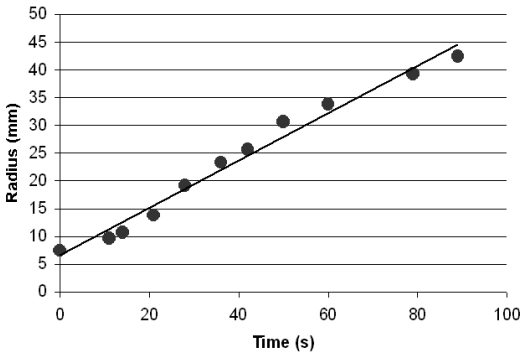

Fig. 9. Plot of the radius of curvature of the electrolysis actuated SBT with respect to time for a constant input current of 100 mA. The data is fit with $R^2 = 0.98$ by $\rho_b = 0.43t + 6.58$.

D. Model Fitting

Since the model and the experimental data have the same basic shape (as shown on Fig. 8), the next task is to fit the model's lumped stiffness parameter K to the experimental data. We measure ρ_b instead of ρ_m, because the bottom boundary of the SBT can be more reliably discerned in video images than the midline. Rearranging the system (2) we obtain,

$$\rho_b = \left(\frac{2L_b}{L_t - L_b}\right)\frac{a_0}{K}p + 2b_0\left(\frac{L_b}{L_t - L_b}\right) = \frac{r_b a_0}{K b_0}p + r_b. \qquad (6)$$

where r_b is the initial radius of curvature of the bottom surface.

As mentioned previously we have applied least squares to the experimental data to obtain $\rho_b = 0.57p + 11.78$. Using measured values of $a_0 = 3.5$ *mm* and $b_0 = 1$ *mm*, we obtain $K = 72.33$ *kPa*.

E. Charge and Curvature

In addition to determining model parameters, we also desire an input-output (charge-curvature) relationship, since charge is the true input to the system. By modulating the current (i) during the time (t) of actuation, we can directly control the charge (q) delivered by the power source to the electrolysis chamber ($q = \int_0^t i\,dt$). By Faraday's law, the number of moles (n) of gas produced by electrolysis is proportional to charge delivered (see Chemical Equation 1). For a constant current $n = it/zF$ where i = 100 mA, z = 4/3, and F = 96485 C, are the current, number of electrons exchanged in electrolysis per mole of products, and Faraday's constant, respectively. Data extracted is depicted in Fig.10 and shows a linear relationship between the pressure produced inside the SBT and the charge delivered. The least squares linear fit is $p = 4.29q$ with R^2=0.95.

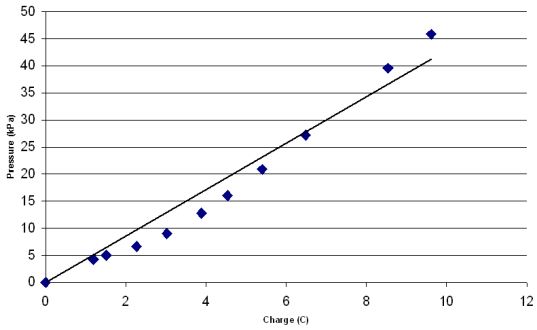

Fig. 10. Radius of curvature vs. the charge delivered at the electrodes. An approximately linear relationship exists with R^2=0.95

V. DISCUSSION

Perhaps the most obvious concern with any electrolysis actuated robot is the non-reversibility of the electrolysis reaction. However, this is one area where the environment of the stomach is actually beneficial for us. The stomach can be filled with water (by simply having the patient drink water before and/or after swallowing the robot modules

[5]). This provides our robots with an aqueous environment, which serves as a vast source of fuel for the electrolysis reaction. We envision small valves embedded in wall of the electrolysis chamber that eject gas when the SBT is depressurized, and then capture water from the environment in preparation for the next actuator cycle. Releasing spent gas in this manner will cause no harm to the stomach or GI, since the gas can easily be vented from the stomach through normal biological processes. We do not anticipate any danger to the patient from ejection of spent oxygen and hydrogen gas, since the small size of the final device will result in small quantities of gas which pose no danger to the patient.

Another exciting topic of future research is the possibility of collecting the hydrogen and oxygen generated and using them to power a second stage actuator. In fact it has been demonstrated feasible to recover some of the energy spent to decompose water in electrolysis using fuel cell technology [8], which generates electricity and produces water as exhaust. Such systems, called regenerative fuel cells, reduce the volume of gas using catalyst mediated recombination of oxygen and hydrogen. Unfortunately, this technology still presents poor scalability because it requires high surface area catalysts (proton exchange membranes) and the separation of the two gas species.

Binary actuation is also an attractive possibility for small modular endoluminal robots, potentially assisting in the path planning and kinematics problems of configuring the larger modular robot into suitable shapes for specific surgical interventions. Our system (as well as other small chambers pressurizable via electrolysis, such as small linear actuators), is amenable to such kinematic frameworks, since we can provide the starting pre-pressurized configuration and the ending post-pressurized configuration. However, further experiments regarding both the stiffness and force generated in various directions at the end of the tube are necessary to enable such path planning and kinematic analyses.

However, as we have shown in this work, the SBT exhibits remarkable linearity with respect to both pressure and charge applied, due geometric effects being dominant over other potentially nonlinear factors. The effect of geometry (as modelled in this paper) is the relationship between the cross sectional profile change and the resulting axial SBT curvature change. Other potential sources of nonlinearity do not appear significant enough over the ranges of motion considered in this paper to cause the SBT to deviate significantly from the basic linear profile predicted by the geometry. .

We expect detailed analysis of the nonlinear factors to require numerical or finite element models because of the complexity involved, which is in addition to the basic complexity analyzing ideal bourdon tube behavior itself. Complete analysis of these factors (as well as complete uniformity in manufacturing procedures) will be necessary only if the required accuracy of tip position or tip force application is very high, or the desired tip travel is very long.

VI. CONCLUSIONS

The prototype of the electrolytically Actuated Silicone Bourdon Tube presented here combines two different well established principles to create a new, scalable microactuator, operating at reasonable bandwidth and very low power. Future work will focus on improving manufacturing processes, miniaturization, more detailed models, and integration of the actuator into a complete modular surgical robotic system for the stomach/GI tract. The remarkable performance of the SBT in terms of linearity, velocity of radius change (0.43 mm/s) and stroke length ($\Delta\rho_b = 35\ mm$) make the electrolytically actuated Silicon Bourdon Tube a very promising potential microactuator for assemblable, reconfigurable, medical robots.

VII. ACKNOWLEDGMENTS

The authors gratefully acknowledge Dr. Samuele Gorini for the helpful discussions and suggestions on silicone properties and treatments.

REFERENCES

[1] N. Patronik, M.A. Zenati, and C. Riviere, "Crawling on the Heart: A Mobile Robotic Device for Minimally Invasive Cardiac Interventions", *in Proc of 7th International Conference Medical Image Computing and Computer-Assisted Intervention 2004*, Part II, Saint-Malo, France, September 26-29, 2004, pp. 9-16.

[2] P. Berkelman, P. Cinquin, J. Troccaz, J. Ayoubi, C. Letoublon, and F. Bouchard, "A compact, compliant laparoscopic endoscope manipulator", *in Proc. of IEEE International Conference on Robotics and Automation 2002*, vol. 2, Washington, DC, USA, May 11-15, 2002, pp. 1870-1875.

[3] B.L. Davies, "Robotic surgery: at the cutting edge of technology", *in Proc. of 7th International Workshop on Advanced Motion Control 2002*, Maribor, Slovenia, July 3-5, 2002, pp. 15-18.

[4] R.H. Taylor, P. Dario, and J. Troccaz, Special issue: Medical Robotics, *IEEE Transactions on Robotics and Automation*, Vol. 19, Issue 5, October 2003.

[5] A. Cuschieri, MD, ChM, FRCSEng, F Med Sci, F Inst Mech Eng (Hon), Personal communication

[6] E.H. Østergaard, K. Kassow, R. Beck, and H.H. Lund, Design of the ATRON lattice-based self-reconfigurable robot, *Autonomous Robots* vol.21, no. 2, September 2006, pp. 165183.

[7] E. Yoshida, S. Kokaji, S. Murata, K. Tomita, and H. Kurokawa, Miniaturization of Self-reconfigurable Robotic System using Shape Memory Alloy Actuator, *Journal of Robotics and Mechatronics*, Vol.12, No.2, 2000, pp. 96-102.

[8] C.G. Cameron and M.S. Freund, Electrolytic actuators: Alternative, high-performance, material-based devices, *PNAS*, vol. 99, no. 12, June 11, 2002 pp 7827-7831.

[9] C. Pang, Y-C. Tai, J.W. Burdick, and R.A. Andersen, Electrolysis-based diaphragm actuators, *Nanotechnology* no. 17, 2006, pp. S64S68.

[10] C. D. Conway, Analytical Analysis of Tip Travel in a Bourdon Tube, *Master Thesis*, Naval Postgraduate School, December 1995.

[11] D. Accoto, D. Campolo, P. Castrataro, V. Surico, E. Guglielmelli, and P. Dario, "A soft electrochemical actuator for biomedical robotics", *in Proc. of IEEE International Conference on Robotics and Automation 2002*, Barcellona (ES), April 18-22, 2005, pp. 2926-2931.